CrossMark

Chemical, thermal and rheological properties and stability of sapucaia (*Lecythis pisonis*) nut oils

A potential source of vegetable oil in industry

Gerson Lopes Teixeira[1] · Suelen Ávila[1] · Joana Léa Meira Silveira[2] ·
Marcelo Ribani[3] · Rosemary Hoffmann Ribani[1]

Abstract Sapucaia (*Lecythis pisonis*) is a tree that grows in Colombia, Venezuela and the Guyanas and is widely distributed in Brazil. This work presents a study of sapucaia nut oils (SO) that were obtained by Bligh and Dyer (LP1) and Soxhlet (LP2) methods and were evaluated for their fatty acid composition, rheological and thermal properties, total phenolic compounds (TPC), antioxidant properties and oxidative stability using Rancimat and ATR-FTIR spectroscopy. The analyses showed that the method of extraction impacts the fatty acid profiles of SO. Oil extracts present considerable TPC content and antioxidant properties. Thermal analysis revealed three degradation steps for SO in the air atmosphere, starting at around 130 °C, being thermally stable up to 300 °C (with a $\sim$ 5% mass loss) and reaching total degradation near 620 °C. Thermal analysis under N_2 produced two degradation steps, initiating at around 130 °C and finishing at 500 °C. Rancimat also confirmed the high thermal stability of SO, with induction periods of 13.28 h (LP1) and 7.18 h (LP2). The DSC parameters of SO were similar among each other. Crystallization (-8.04 to -73.93 °C) and melting (-31.34 to 8.28 °C) phases occurred over a large temperature range. SO presented FTIR spectral features with characteristic bands for vegetable oils. Ostwald–de Waele and Herschel–Bulkley rheological models indicated major pseudoplastic behavior for SO, with a predominant viscous component. These results reinforce that SO are appropriate for human consumption and open up new possibilities for their industrial exploitation, such as for food and the cosmetic, pharmaceutical and biodiesel industries.

Keywords *Lecythis pisonis* · Oil · Fatty acids · Stability · Thermal analysis · Rheology

Abbreviations

SO	Sapucaia nut oil (s)
LP1	Oil extracted by Bligh and Dyer
LP2	Oil extracted by Soxhlet
TPC	Total phenolic compounds
Trolox	6-Hydroxy-2,5,7,8-tetramethylchroman-2-carboxylic acid
TPTZ	2,4,6-Tri(2-pyridyl)-*s*-triazine
DPPH	1,1-Diphenyl-2-picrylhydrazyl
ABTS	2,2′-Azino-bis(3-ethylbenzothiazoline-6-sulfonic acid)
FRAP	Ferric reducing antioxidant power
TE	Trolox equivalent
GA	Gallic acid
GAE	Gallic acid equivalents
OSI	Oxidative stability index
IP	Induction period
ATR-FTIR	Attenuated total reflectance Fourier transform infrared spectroscopy
FA	Fatty acid
SFA	Saturated fatty acid
UFA	Unsaturated fatty acid
MUFA	Monounsaturated fatty acid
PUFA	Polyunsaturated fatty acid

✉ Gerson Lopes Teixeira
gerson775@gmail.com

[1] Graduation Program of Food Engineering, Polytechnic Center, Federal University of Paraná, Jardim das Américas, P.O. Box 19011, 81531–990 Curitiba, Paraná, Brazil

[2] Department of Biochemistry and Molecular Biology, Polytechnic Center, Federal University of Paraná, Jardim das Américas, 81531-980 Curitiba, Brazil

[3] Paraná Institute of Technology, João Américo St, 500 Curitiba, Brazil

Springer

TAG   Triacylglycerol
SFC   Solid fat content
OW   Ostwald–de Waele
HB   Herschel–Bulkley

Introduction

The search for new crops to provide vegetable oils for use in industry and for human consumption has been increasing over the past two decades. A search on the Web of Science[TM] platform produces more than 19,200 results related to "nuts," more than 7600 documents are related to "edible oils," and more than 22,000 results are associated with "vegetable oil." The published items regarding vegetable oil increased from 282 in 1996 to more than 1930 in 2016, illustrating the growing interest of the scientific community in this field of study [1].

Several types of Brazilian seed and nut, especially from the Amazonian area, have been studied during recent years, and most species were shown to present bioactive compounds and potential as functional foods [2–7]. Other species are not well known or have not been submitted to any further study to elucidate their characteristics.

Lecythis pisonis Camb., a Lecythidaceae tree that grows in Brazil, Colombia, Venezuela and the Guyanas, commonly known as "sapucaia," produces nuts that are similar to Brazil nuts (*Bertholletia excelsa*). The edible kernels of sapucaia have a characteristic sweet flavor and are considered more digestible than Brazil nuts [8]. In addition to the economic and ecological importance of sapucaia, which is often used to shade cocoa plantations in Brazilian agroforestry systems [9], the nuts from *L. pisonis* are a valuable source of macro- and micronutrients, essential amino acids, minerals such as P, K, S, Mg, Ca, Mn, Ba, Zn, Fe, Sr, Cu, B, Al and Cl [3, 10] and fibers [11]. The proximate composition of sapucaia nuts is presented in Table 1, which shows different compositions according to different authors; the content of protein can vary from 18 to 26%, while carbohydrates range from 5 to 11%. Furthermore, lipids constitute 51–64% of the composition of sapucaia nuts [5, 8, 10, 11], and of these, linoleic acid (an essential fatty acid) is predominant. Although sapucaia could potentially be a crop to provide raw material for the production of vegetable oil, the studies that have been conducted on these nuts have mostly focused on their mineral and fatty acid profiles [3, 5, 10, 12, 13] and the latest reports are limited to agronomic, microbial and pharmacological aspects [9, 14–17].

Vegetable oils are widely utilized in the food, cosmetic, pharmaceutical and biofuel industries. Consequently, stability tests, rheological assays and phase transitions should be conducted in order to optimize processing conditions and energy inputs [18, 19]. No reference has been found regarding the total phenolic compounds, antioxidant activity or thermal and rheological characterization of sapucaia nut oil. Therefore, the aim of this work was to extract sapucaia nut oils using the Soxhlet and Bligh and Dyer methods and to evaluate the oils for their fatty acid composition, rheological behavior and thermal properties using differential scanning calorimetry (DSC) and thermogravimetry (TG) analysis, total phenolic compounds (TPC), antioxidant properties and oxidative stability using Rancimat and attenuated total reflectance Fourier transform infrared spectroscopy (ATR-FTIR).

Materials and methods

Chemicals

Folin–Ciocalteau reagent, Trolox (6-hydroxy-2,5,7,8-tetramethylchroman-2-carboxylic acid), TPTZ (2,4,6-tri(2-pyridyl)-s-triazine), DPPH (1,1-diphenyl-2-picrylhydrazyl), ABTS (2,2′-azino-bis(3-ethylbenzothiazoline-6-sulfonic acid)), gallic acid (GA, $\geq$ 98.0%) were purchased from Sigma-Aldrich (St. Louis, Mo, USA). Other reagents used in the experiments were of analytical grade. The aqueous solutions were prepared using ultrapure water.

Samples

Sapucaia (*Lecythis pisonis*) nuts were harvested in the season of August 2016, from a crop area located in the city of Araguanã, Maranhão State, Brazil. The nuts (Fig. 1) were dried in an air-circulating oven (40 °C for 24 h). Nut shells were removed manually using a stainless-steel knife and then freeze-dried (Liotop L101, Liobras, Brazil). Residual moisture in the samples was 4.07 $\pm$ 0.90%. Prior to oil extraction, the nut samples were crushed for 30 s with the aid of a stainless-steel knife grinder (MA630/1, Marconi Ltda., Brazil).

Table 1 Proximate composition of *Lecythis pisonis* nuts according to different authors

Characteristic	a[*]	b[*]	c[**]
Moisture/%	3.2 $\pm$ 0.16	10.20 $\pm$ 0.68	4.95
Ash/%	3.1 $\pm$ 0.25	3.17 $\pm$ 0.50	3.91
Lipids/%	64.0 $\pm$ 2.35	54.80 $\pm$ 4.15	63.03
Protein/%	18.5 $\pm$ 0.97	26.82 $\pm$ 2.60	19.86
Total fiber/%	7.0 $\pm$ 0.77	–	–
Total carbohydrates	11.1 $\pm$ 2.13	5.01[3]	8.28

a = Carvalho et al. [11]; b = Carvalho et al. [12]; c = Vallilo et al. [10]

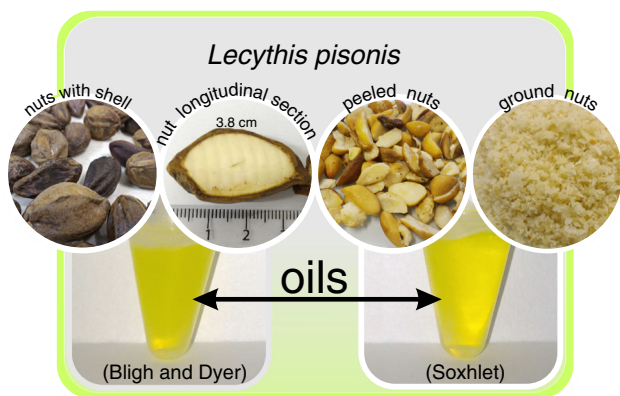[*]Result expressed as the average $\pm$ standard deviation (SD)

[**]No SD

Fig. 1 Sapucaia (*Lecythis pisonis*) nuts and oils

Extraction of nut oils

The oil content of *L. pisonis* nut samples was extracted using the Bligh and Dyer method described in the American Oil Chemists' Society (AOCS) Official Method Ba 3-38 and also using *n*-hexane with the Soxhlet apparatus (Vidrolabor®, Labor Quimi, Brazil) [20]. The oils were named LP1 and LP2, respectively. After the oil extraction, solvents were removed at 43 °C under reduced pressure using a rotary evaporator (Model 801, Fisatom Ltda., Brazil). Samples were dried at 45 °C in an air-circulating oven (Solab, Brazil) for 2 h and then flushed with gaseous N_2 before storage. Samples yielded 49.50 ± 0.50% (LP1) and 55.20 ± 0.10% (LP2) of oil. The oils were kept in amber glasses and stored at − 10 °C until further analysis.

Analytical determinations

Water content and apparent pH

Water content was measured by volumetric Karl Fischer titration using a titration system (V30 Mettler-Toledo, Switzerland) [21]. The pH was determined according to the method of Pena Muniz et al. [22], as recommended by the Brazilian National Agency for Sanitary Surveillance, without previous dilution of the oil, with the aid of a digital pH meter (Model PG1800 Gehaka) at 25 ± 2 °C. The results represent the mean of three measurements.

Fatty acid composition

The fatty acid composition of fresh *L. pisonis* oils was investigated using the AOCS Official Method Ce 1a-13 [20] with a GC–MS system (GC-2010) coupled to a mass spectrometer (GCMS-TQ8030) and automatic injection system by headspace (Shimadzu, Japan). Oil samples solubilized with hexane were methylated as described by

AOCS Ce 2-66 and then injected into a capillary HP88 column (60 m × 0.250 mm i.d., 0.2 μm film thickness, Agilent Technologies) using helium as the carrier gas (0.64 mL min^{-1}). The oven temperature was programmed to be 175 °C (isothermal), and the detector was held at 250 °C. A 1μL aliquot of the sample was injected using the split injection mode (1:100). Fatty acid composition was expressed as the percentage of the total peak area of all the fatty acids in the oil sample.

Rheological characterization

Rheological measurements of oils were taken according to Teixeira et al. [19], by using a Haake Mars II (Thermo Electron GmbH, Germany) rheometer with a sensor cone plate (C60/2°Ti L; 60 mm diameter, 2° cone angle). The calculated measurements were: (a) flow curve ($\dot{\gamma} = 0.01$–500 s^{-1}, $t = 300$ s); (b) dynamic stress sweep ($\tau = 0.01$–100 Pa, $\omega = 1$ Hz) and subsequent dynamic frequency sweep ($\omega = 0.1$–100 Hz, $\tau = 1.0$ Pa); (c) temperature sweep ($T = 10$–60 °C, 2 °C min^{-1} and 60–10 °C, 5 °C min^{-1}; $\omega = 1$ Hz, $\tau = 1.0$ Pa). The samples were covered with a sample hood in order to avoid interference from the ambient temperature.

The coefficient of determination (R^2) and Chi-square (χ^2) was chosen to evaluate the fit of the Ostwald–de Waele (Eq. 1) and Herschel–Bulkley (Eq. 2) models to the experimentally obtained flow curves:

$$\tau = K\dot{\gamma}^n \text{—Ostwald-de Waele (OW)} \tag{1}$$

$$\tau = \tau_{0H} + K_H(\dot{\gamma})^n H \text{—Herschel-Bulkley (HB)} \tag{2}$$

where τ is the shear stress (Pa), $\dot{\gamma}$ is the shear rate (s^{-1}), τ_{0H} is the HB yield stress (Pa), K and K_H are the consistency indices (Pa·s^n) and n and n_H are the flow behavior indices (dimensionless).

The effect of temperature on apparent viscosity was evaluated according to an Arrhenius-type equation (Eq. 3), using a shear rate of 53.4 s^{-1}.

$$\eta = \eta_0 \exp\left(\frac{E_a}{RT}\right) \tag{3}$$

where η is the apparent viscosity at a specific shear rate, η_0 is the pre-exponential factor, E_a is the activation energy (J mol^{-1}), R is the gas constant (8.31 J K^{-1} mol^{-1}) and T is the absolute temperature (K).

Oxidative stability index

The oxidative stability index (OSI), also called induction period (IP), was estimated in a Metrohm Rancimat model 743 (Herisau, Switzerland), following the AOCS Official Method Cd 12b-92 [20]. Briefly, increasing water

conductivities were continually measured, while air (20 L h^{-1}) was bubbled into the oil (3 ± 0.1 g), which was heated to 110 °C, and the volatile compounds were collected in water. The time taken to reach the conductivity inflection point was recorded. The IP was registered by Rancimat 743 PC Software 1.1.

Infrared spectroscopy

Fourier transform infrared spectroscopy (FTIR) analysis was performed using a Vertex-70 spectrometer (Bruker, USA) with an attenuated total reflectance (ATR) accessory, at 25 °C. The oil samples were placed uniformly in the ATR crystal (1.5 mm active area). The FTIR spectra were recorded in the wave number range of 4000–600 cm^{-1} with a spectral resolution of 4 cm^{-1}.

TG/TGA thermal decomposition

TGA analyses were performed with TGA 4000 equipment (PerkinElmer Inc. Waltham, USA). An oil sample (∼ 10 mg) was placed into the platinum pan and then into a furnace. The sample was heated from 30 to 750 °C (10 °C min^{-1}) in the air atmosphere (70 mL min^{-1} flow rate) or under a nitrogen atmosphere. Data on the mass changes of oil samples were obtained using Pyris^{TM} software. TG and derivative thermogravimetric (DTG) curves were further analyzed using Origin 8.6 software (OriginLab, Massachusetts, USA). The thermal stability was measured from the extrapolated onset temperature of the first step of thermal decomposition from the respective TG curves. The beginning and the peak temperature of the respective DTG peaks were used as the temperature limits for the data analysis software of the instrument.

DSC analysis

For DSC analysis, a DSC 8500 (PerkinElmer Inc. Waltham, USA) was used. Nitrogen (99.99% purity, White Martins, Brazil) was the purge gas (20 mL min^{-1}). The DSC instrument was previously calibrated with indium (m.p. 156.6 °C, $\Delta H = 28.45$ J g^{-1}). The sample was weighed into an aluminum pan and sealed. An empty, hermetically sealed, aluminum sample pan was used as the reference. In order to reduce temperature gradients, the sample mass was kept small (∼ 9.0 mg). The methodology applied was adapted from Zhang et al. [23]. To produce cooling and melting curves, the samples were first rapidly heated to 80 °C (30 °C min^{-1}) from room temperature and held for 10 min. Then, the samples were cooled to − 80 °C (10 °C min^{-1}) and held for 10 min to ensure they became fully crystallized and then heated to 80 °C (5 °C min^{-1}). To study the effect of the cooling rate on crystallization, samples were rapidly heated to 80 °C (30 °C min^{-1}) from room temperature and held for 5 min, and then, the samples were cooled to − 80 °C at the cooling rates of 2, 5 or 10 °C min^{-1}. To investigate the melting profile of L. pisonis oils under isothermal crystallization, the samples were heated at 80 °C (30 °C min^{-1}) for 5 min and then cooled (100 °C min^{-1}) to a preset temperature (− 10, 0, 10, 20 °C), held at that temperature for 10 min for crystallization and then heated to 80 °C (5 °C min^{-1}). Pyris^{TM} manager software was used to calculate the parameters of crystallization and melting, enthalpies and the solid fat content (SFC), which was estimated based on the integrated area under the melting curve [24].

Total phenolic compounds

The total phenolic compounds (TPC) were determined in methanolic extracts of vegetable oils [25], using 1.0 g of oil. Briefly, for extraction of oils, 90:10 methanol/water (3 mL) was added, followed by vortex mixing for 4 min and centrifugation for 5 min at 15,000 u min^{-1}. The extraction procedure was carried out three times for each oil. All methanolic extracts were combined and analyzed sequentially using the Folin–Ciocalteu reagent assay. The quantification of TPC was performed using the microplates technique [26], with gallic acid as a standard for the calibration curve. The absorbance at 720 nm was measured using a spectrophotometer (Tecan Nanoquant Infinite® M200, Tecan Trading AG, Switzerland) after reaction with the Folin–Ciocalteu reagent in the alkaline medium and standing in the dark for 1 h. TPC were expressed in mg of gallic acid equivalents (GAE)/100 g of oil.

Antioxidant assays of the oil extracts

The free radical scavenging evaluated by the DPPH assay was determined using the method proposed by Brand-Williams et al. [27]. The absorbance at a wavelength of 517 nm was measured using a spectrophotometer (Tecan Nanoquant Infinite® M200, Tecan Trading AG, Switzerland). The ABTS scavenging activity of oil extracts was determined in triplicate using the method described by Re et al. [28]. The absorbance at 734 nm was measured. The total antioxidant potential of the oil extracts was measured using the ferric reducing antioxidant power (FRAP) assay [29]. Measurements were taken using the spectrophotometer at 593 nm. The absorbance of the samples was compared to a standard curve (100–1000 μmol L^{-1}), and results were expressed in mmoL Trolox equivalent per g of oil (mmol TE g^{-1}). All the assays had minor changes as proposed by Zielinski et al. [30].

Data analysis

Origin 8.6 software (OriginLab, Massachusetts, USA) was used for data treatment and producing graphs. Statistica 10.0 (Statsoft, Brazil) was used for statistical analysis, including calculating means and standard deviations (SD). All experiments were carried out in triplicate.

Results and discussion

Water content and apparent pH

Commonly, the water content in vegetable oils is less than 1%. As expected for this type of raw material, sapucaia oil (SO) samples presented very low water content: $0.077 \pm 0.006\%$ for LP1 and $0.097 \pm 0.006\%$ for LP2. The low moisture content helps the oil to maintain good properties against oxidation. This result is similar to that of Brazil nut oil ($< 1.0\%$) [22], pequi oil (0.07%) [31] and canola oil ($< 0.3\%$) [32]. The apparent pH of SO was 5.720 ± 0.036 for LP1 and 5.353 ± 0.040 for LP2, lower acid than Brazil nut oil (3.80) [22].

Phenolic compounds and antioxidant properties

Seeds are naturally rich sources of phenolic compounds, which can easily end up in the resulting extracted oil [33]. The studied sapucaia nut oils presented a considerable amount of phenolics, with different values ($p < 0.05$) varying according to the method of extraction (Table 2). The oil sample LP1 presented higher TPC content than that of LP2. The content of phenolic compounds present in the SO (1.418 mg GAE/100 g on average) is greater than in almond oil (0.95 mg GAE/100 g), similar to hazelnut oil (1.59 mg GAE/100 g) and pine nut oil (1.48 mg GAE/100 g); however, Brazil nut oil appears to show similar (1.53 mg GAE/100 g) [34] or twice the TPC content (3.64 mg GAE/100 g) of SO, and macadamia nut oil presents fifteen times more TPC (22.5 mg GAE/100 g) [35].

Elucidating the antioxidant profile of edible oils is important because the antioxidants are associated with suppress, delay of avoid harmful oxidation processes, principally the ones caused by reactive oxygen species, playing a crucial role in the shelf life, nutritional value and quality of the food products, and serving as a quality index [36]. The antioxidant activity of the phenolic extracts from SO was evaluated by three different methods, and the results are shown in Table 2.

The oils presented radical-scavenging activities suggesting that they can inhibit free radicals in vivo. According to the data, no significant difference ($p < 0.05$) was observed between the results from DPPH and FRAP assays. However, the ABTS assay showed that the sample LP1, which was obtained by a cold extraction process, has better antioxidant characteristics than LP2. Another study agrees with our results, where various nut oils such as Brazil nut, pecan, hazelnut, pistachio, walnut and almond oils extracted by chloroform/methanol (as Bligh and Dyer method) present higher antioxidant activity compared to hexane-extracted oils [34]. The numerical value from ABTS analysis is usually higher than the DPPH assay, as shown by Christodouleas et al. [36], which also showed that ABTS method presents higher sensitivity for hydrophilic compounds extracted from oilseeds over DPPH, although both methods have comparable results. In addition, Table 2 shows that SO had effective reducing power using the FRAP method, which measures both water- and fat-soluble antioxidants [37], showing no difference ($p < 0.05$) between the analyzed samples, thus demonstrating that the electron donor properties of SO can neutralize free radicals by forming stable products. According to Blomhoff et al. [37], the FRAP assay has the advantage to directly measure antioxidants or reductants in a sample, while the other methods are more indirect, measuring the inhibition of reactive species produced in the reaction mixture.

Some natural antioxidants, which are responsible for protecting biological systems from reactive oxygen species, are commonly present in vegetable oils as phenolic compounds, carotenoid compounds, phytosterols and tocopherols (vitamin E) [38], and may also have influenced the antioxidant capacity of SO, being possible to make a relationship between them [39]. The results from in vitro antioxidant assays presented some variations that could be assigned to the different mechanisms in the analysis (Table 2). These assays are grouped into the electron-transfer category, and there is some specificity among them. DPPH and ABTS radical cations have the same mechanism and produce a characteristic color that can be monitored by a

Table 2 Total phenolic compounds (TPC) and antioxidant activity of sapucaia oils measured by different methods

Sample	TPC/mg GAE/100 g	DPPH[a]	ABTS[a]	FRAP[a]
LP1	1.590 ± 0.087^a	3.429 ± 1.866^a	8.715 ± 0.293^a	26.148 ± 0.150^a
LP2	1.246 ± 0.026^b	1.973 ± 0.727^a	5.585 ± 0.385^b	25.760 ± 0.385^a

Values are the mean $\pm$ standard deviation. Means followed by same letter do not differ by Duncan test ($p < 0.05$). GAE gallic acid equivalents

[a] Results in mmol Trolox equivalent per g of oil (TE/g oil)

spectrophotometer. The color change occurs when the oil extract is mixed with a reactant solution and the reduced form of the radical loses its color as a result of donating a hydrogen atom. Similarly, in the presence of antioxidant compounds, FRAP is characterized by electron-transfer ability that results in the reduction in iron ions [33, 36, 40].

Fatty acid profile

Fourteen different fatty acids (FAs) were identified in the studied SO (Table 3). The oils were composed predominantly (61–73%) of unsaturated fatty acids (UFAs). Monounsaturated fatty acids (MUFAs) accounted for 39.08–45.66%, and 21.95–27.63% was polyunsaturated fatty acids (PUFAs), such as linoleic and α-linolenic acids, which have been proven to effectively reduce the risk of cancer, osteoporosis, cardiovascular diseases and diabetes [41]. Such a FA profile is common for Brazilian edible nuts [5, 42], which reinforces the idea that consuming more nuts rich in fatty acids is beneficial to health. Currently, the main commercial source of PUFA, such as ω-3 and ω-6, is fish and fish fat [41].

Among the MUFAs, oleic acid was the major FA found in SO, which accounted for 44.28% in LP1 and 35.54% in LP2. It is important to note that oleic acid is the primary ω-9 FA in the human diet and is the predominant MUFA in many nut oils, totaling 38.50% in Brazil nut oil (*Bertholletia excelsa*) [22], 65.59% in garampara oil (*Dipteryx lacunifera*) [5], 67.62% in tucumã oil (*Astrocaryum vulgare* Mart.) and 39.04% in cutia nut oil (*Couepia edulis*) [42]. The SO also contained 21.65–27.19% linoleic acid, an essential FA that, in reasonable amounts, is important for human health [43]. The SO also contained two important *cis*-MUFA, the *cis*-vaccenic and *cis*-11-eicosenoic in quantities higher than 1.0%.

The saturated fatty acids (SFAs) represented 25.01–37.25% of the total FA and were mainly palmitic acid (14.70–21.38%) and stearic acid (9.63–11.09%). Other SFA such as myristic, heptadecanoic and behenic acids were identified in smaller amounts. Arachidic acid, which is usually present in peanut oil, was also found in SO in small quantities; this result is in agreement with Costa and Jorge (2012), who found about 0.22% C20:0 for *L. pisonis* oil. There is a similar pattern in the Brazil nut oil, which contains 0.36% arachidic acid and 14.26% palmitic acid [22].

A good factor for evaluating the quality and digestibility of a vegetable oil is the amount and composition of UFA and SFA. A high amount of linoleic acid in comparison with oleic acid (ω-9) represents better quality vegetable oil [5]. The relationship between linoleic and oleic acids should, therefore, be considered when assessing oil. Oils can present diverse values for these relationships depending on the extraction method, as shown in Table 4, where sapucaia oils

Table 3 Fatty acid profile of sapucaia oils in comparison with other studies

Fatty acids/%	LP1	LP2	*a*	*b*
Myristic (C14:0)	0.12	0.23	–	–
Palmitic (C16:0)	14.70	21.38	14.49	10.68
Heptadecanoic (C17:0)	0.11	0.17	–	–
Stearic (C18:0)	9.63	11.09	5.84	5.63
Arachidic (C20:0)	0.45	0.38	0.22	–
Behenic (C22:0)	nd	3.99	tr	–
ΣSFA	25.01	37.25	20.76	16.30
Palmitoleic (C16:1)	0.32	0.44	0.21	–
Elaidic (C18:1 n9t)	nd	0.04	–	–
Oleic (C18:1 n9c)	44.28	35.54	38.82	34.30
cis-Vaccenic (C18:1 n11c)	1.05	1.24	–	–
cis-11-Eicosenoic (C20:1 n9)	nd	1.87	–	–
ΣMUFA	45.66	39.08	39.07	–
Linoleic (C18:2 n6c)	27.19	21.65	39.93	49.35
α-Linolenic (C18:3 n3)	0.36	0.29	0.24	–
Arachidonic (C20:3 n3)	0.08	nd	–	–
ΣPUFA	27.63	21.95	40.18	–
Others	–	–	0.24	–
ΣTotal UFA	73.29	61.02	79.25	83.65

nd not detected, *tr* traces, *SFAs* saturated fatty acids, *MUFAs* monounsaturated fatty acids, *PUFAs* polyunsaturated fatty acids

a = Costa and Jorge [5]; *b* = Vallilo et al. [10]; results are expressed as % distribution of fatty acids

present UFA/SFA and linoleic/oleic FA ratios ranging from 1.63 to 5.13 and 0.609 to 1.44, respectively. Results highlighted that SO present high UFA/SFA relationship regardless of the extraction process; on the other hand, the linoleic/oleic FA ratio is highly affected by the extraction method and presents lower values when extracted by Bligh and Dyer and Soxhlet with hexane. It is also shown that SO has better characteristics according to the method of extraction as the following sequence: Soxhlet with petroleum ether > cold press > Bligh & Dyer > Soxhlet with hexane. Both relationships for sapucaia oils in the current study are lower than those found by Costa and Jorge (2012) and Vallilo et al. (1999) because the oils produced in these studies had a higher linoleic acid content (Table 3). When compared to other Brazilian oleaginous nuts such as the Brazil nut, garampara [5] and cutia nut [42], the unsaturation relationship values between linoleic and oleic acid were also quite different. The results revealed that that method of extraction highly impacts the composition of sapucaia oil and, consequently, the quality characteristics.

Oxidative stability index

The oxidative stability index (OSI) is an important part of evaluating oil quality. The OSI was evaluated with

Table 4 Comparison of unsaturated fatty acid composition of sapucaia oils and other Brazilian vegetable oils

Vegetable oils	Method of extraction	Relationship between unsaturated and saturated fatty acids	Relationship between linoleic and oleic fatty acids
Sapucaia (*Lecythis pisonis*)[a]	Bligh and Dyer	2.93	0.614
Sapucaia (*Lecythis pisonis*)[a]	Soxhlet with hexane	1.63	0.609
Sapucaia (*Lecythis pisonis*)[b]	Cold pressing	3.82	1.03
Sapucaia (*Lecythis pisonis*)[c]	Soxhlet with petroleum ether	5.13	1.44
Brazil nut (*Bertholletia excelsa*)[b]	Cold pressing	3.05	1.44
Brazil nut (*Bertholletia excelsa*)[d]	Soxhlet with hexane	3.08	1.517
Cutia nut (*Couepia edulis*)[e]	Cold pressing	1.39	0.32
Garampara (*Dipteryx lacunifera*)[b]	Cold pressing	3.45	0.14

[a]This work

[b]Costa and Jorge [22]

[c]Vallilo et al. [10]

[d]Santos et al. [12]

[e]Costa-Singh et al. [42]

Rancimat analysis until the end point of stability for SO samples and was expressed in hours. The higher the OSI, the better the resistance to oxidation and higher is the shelf life of the oil; consequently, an oil with high OSI represents a good source of raw material for the food industry. The oil sample LP1 was the one with highest shelf life, once it presented 13.28 ± 0.22 h for OSI, while LP2 has a lower shelf life, because the OSI was only 7.18 ± 0.50 h. The results confirmed that Bligh and Dyer, which is a cold extraction process, is a technique that causes less damage to the oil than Soxhlet, once the former nearly halved the value of the OSI presented by the latter. The high oleic acid content in SO tends to protect the oil against thermo-oxidation. Another reason for the excellent oxidative stability of sapucaia oils is because of the presence of natural antioxidants and polyphenols, which are present in all vegetable oils [44], as confirmed by the TPC content and antioxidant activity assays, being then responsible for enhancing the resistance to oxidation [32, 36, 44]. Extracts of phenolic compounds are suggested to be added to oils with low oxidative stability aiming to enhance the OSI [33]. Costa and Jorge (2012) found an OSI of 24.89 h (evaluation at 100 °C) for *L. pisonis* oil extracted by cold pressing. At the same Rancimat conditions used in this study, similar results were found for Brazil nut oil (8.24 h), hazelnut oil (8.88 h) and macadamia nut oil (7.38 h) [35].

Thermal decomposition

The thermogravimetric curve (TG) shows the mass loss, and the derivative thermogravimetric curve (DTG) shows the rate of mass loss of SO during thermal decomposition from 30 to 750 °C by TGA under synthetic air (Fig. 2, left images) and under nitrogen (Fig. 2, right images) atmospheres. The values of mass loss are indicated in Table 5. The TG curves indicated that SO were thermally stable up to 303 °C with a mass loss of ∼ 5%. This can be explained by the loss of moisture and volatile compounds in the oils. Under synthetic air, a slight increase (∼ 0.1%) in the sample mass was noticed at the beginning of oxidation (30–76 °C) attributed to the oxygen uptake, and formation of hydroperoxides, causing an earlier decomposition onset than in the nitrogen atmosphere. The oxidative process in vegetable oils is characterized initially by the formation of secondary products (peroxides) through oxidation. The following phase corresponds to the decomposition of MUFA, mainly oleic acid, PUFA (as the linoleic acid) and the polymerization of the substances remaining from the previous phase [45].

Dynamic and inert atmospheres produced different patterns in the TG/DTG profiles. A comparison of the change in mass as a function of temperature is illustrated in Fig. 2e, f where the curves of SO are presented in an overlay, highlighting some differences between samples in each atmosphere. The decomposition and carbonization processes in the air atmosphere occurred in three phases of the curve, starting at around 130 °C, achieving 53–58% mass loss at 405–440 °C and ending at a temperature range of 611–625 °C. For the nitrogen atmosphere, the process showed two steps, initiating at ∼ 160 °C, reaching 62–75% mass loss at 426–435 °C, and finishing at 500 °C. The DTG curves (Fig. 2) showed the steps of thermal decomposition more clearly. At the higher aforementioned temperatures, the mass loss reached 100% (no residue remaining). The high UFA content in SO, mainly oleic acid and linoleic acid, is related to the occurrence of oxidative

Fig. 2 TG/DTG curves of sapucaia oils obtained using the Bligh and Dyer (**a**, **b**) and Soxhlet (**c**, **d**) methods, and a comparison of mass loss as a function of temperature (**e**, **f**) when analyzed under air (left images) and under nitrogen (right images) atmospheres
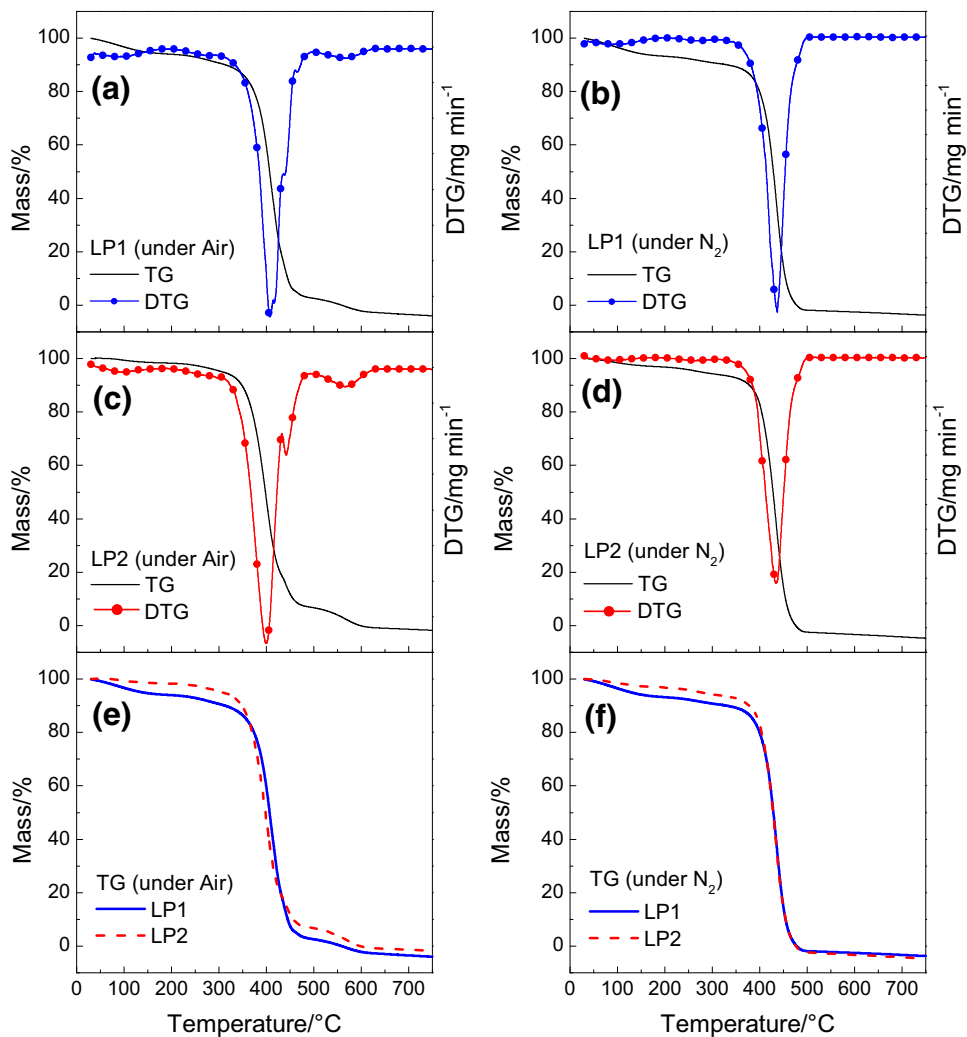

Table 5 TG/DTG data of each thermal decomposition stage of sapucaia oils under flowing air and nitrogen atmospheres

Carrier gas	Sample	Thermal degradation stage	T_i/°C	T_m/°C	T_f/°C	Δm/%
Air	LP1	I	128	362	405	58.2
		II	405	432	545	41.1
		III	545	587	625	0.7
	LP2	I	130	352	392	53.2
		II	392	409	440	34.4
		III	437	464	611	12.4
Nitrogen	LP1	I	160	389	435	75.7
		II	435	450	500	24.3
	LP2	I	162	393	426	62.9
		II	426	445	500	37.1

T_i initial temperature, T_m maximum mass loss temperature, T_f final temperature, Δm mass loss

degradation reactions [22]. The high values of T_i (onset temperature) showed that SO have high thermal stability because of the higher the T_i of decomposition of the oil, the higher the thermal stability. The overall mass of LP1 was different from LP2 in the temperatures ranging from 350 to 550 °C (Fig. 2) possibly due to the high-SFA content (37.25%) in LP2 compared to LP1 (25.01%) [46].

The results are similar to those of Brazil nuts, which are thermally stable up to 209–220 °C and reach a maximum mass loss of 97% at 580–602 °C [22, 45]. Differences between the thermal behaviors of the sapucaia oils can be related to the differences in FA composition and to the presence of natural antioxidants, which tend to protect the oils against oxidation, thus retarding the degradation [47]. In general, vegetable oils present high tocopherol content; while the tocopherol profile of sapucaia nut oil is still unknown, more

research is needed to identify the role of these compounds on the oxidative stability of these oils.

Thermal behavior of crystallization and melting

Temperature for crystallization and the impact of scanning rate

Tests were conducted to investigate the melting profile of SO under isothermal crystallization. The melting thermogram (Fig. 3a, b) revealed that when frozen at − 10 °C the oil samples showed endothermic peaks at − 6.81 °C (LP1) and at − 6.16 °C (LP2), with an enthalpy of 9.28 J g^{-1} for LP1 and 7.26 J g^{-1} for LP2. On the other hand, there was no event after 0 °C, revealing that no crystallization occurred above that temperature. This feature may confirm the liquid state of the SO at room temperature (25 °C).

During cooling, the oils exhibited two transitions. The curves showed that the positions of the exotherms were dependent on the cooling rate, while the quantity of exotherms was independent of the cooling rate. In addition, increasing the cooling rate caused the crystallization peak temperature to shift to lower temperatures and an increase in the peak height and area (Fig. 3c, d). This behavior may correspond to the differential crystallization of higher melting triacylglycerols (TAGs) firstly and lower melting TAGs secondly. Similar results have been described for palm oil fractions [23].

The scanning rate of 2 °C min^{-1} reduces the lag in the output response from the DSC instrument, preserves the minor peaks and reduces the smoothing tendencies, which occurred at a higher scanning rate. However, the first peak

was too small when compared to the rate of 5 °C min^{-1}, which provided better resolution for the peak analysis in the Pyris^{TM} software.

Cooling curve

During cooling (Fig. 4a), both sapucaia oils presented a similar pattern of crystallization, showing two distinct peaks (exothermic) in the crystallization behavior, namely peak 1 (P_{C1}) and peak 2 (P_{C2}). P_{C1} indicated the change from liquid to solid and was found at temperatures of − 11.56 °C (LP1) and − 12.51 °C (LP2), while P_{C2} was observed at temperatures of − 59.80 °C to − 73.93 °C. Both were related to the crystallization of TAGs. The crystallization onset temperature occurred at around − 8.0 °C, and this process extended over a range of 15–23 °C. The sum of the crystallization enthalpy of the two peaks for the two oils was − 22.17 and − 32.56 J g^{-1} for LP1 and LP2, respectively (Table 6). Heat is released during the phase transition of oil from liquid form to solid form so values for crystallization enthalpy were negative [48].

Different endothermic and exothermic peaks are exhibited according to different saturated or unsaturated TAG and FA contents in the oils [49]. Smaller or shoulder peaks are also correlated with different types of TAG. In addition, an inseparable shoulder peak that melts at the same temperature range of the major peak comes from the complex nature of the TAG [50].
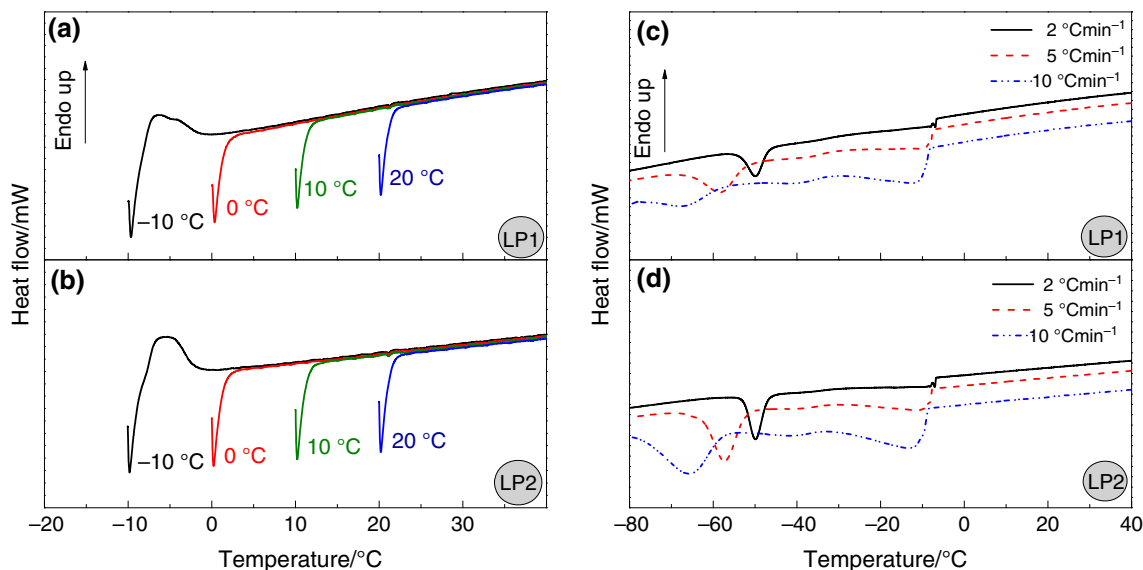

Fig. 3 DSC curves of sapucaia oils. **a**, **b** Melting profile under isothermal crystallization. **c**, **d** The impact of the scanning rates of 2, 5 and 10 °C min^{-1} on crystallization behavior

Heating curve

During melting, SO were found to completely melt at 8.28 and 6.29 °C (LP1 and LP2, respectively) when heated at 5 °C min^{-1} (Fig. 4b). Moreover, LP1 showed a single major shoulder before the maximum melting peaks (P_M) at − 18.42 °C, while LP2 showed a major shoulder before P_M (− 21.47 °C) and an additional one after the major peak at − 6.61 °C. The melting curve of SO began at − 25.77 °C (LP1) and − 29.87 °C (LP2), and the major peak was observed in the temperature region of − 7.99 °C to − 10.13 °C; the events ended at around − 1.09 °C to − 1.68 °C, revealing that this region comprehends the melting point of the SO. The process comprised a melting range of 24–28 °C, with a melting enthalpy of 59.34 J g^{-1} (LP1) and 64.76 J g^{-1} (LP2) (Table 6). The low melting point of an oil is highly related to the degree of unsaturation of the FA, due to the lower melting points of TAGs formed by UFA. This also reinforces that more research about the TAG composition of SO is required to assess the role of this components in its thermal behavior, once TAGs with the same fatty acids can show different properties according to the position of each FA in the glycerol structure (isomerism).

In the heating treatment of oil, multiple endothermic regions are correlated with the separate melting events of the TAG. Furthermore, the composition and polymorphism of the oils can cause some overlapping effects, resulting in
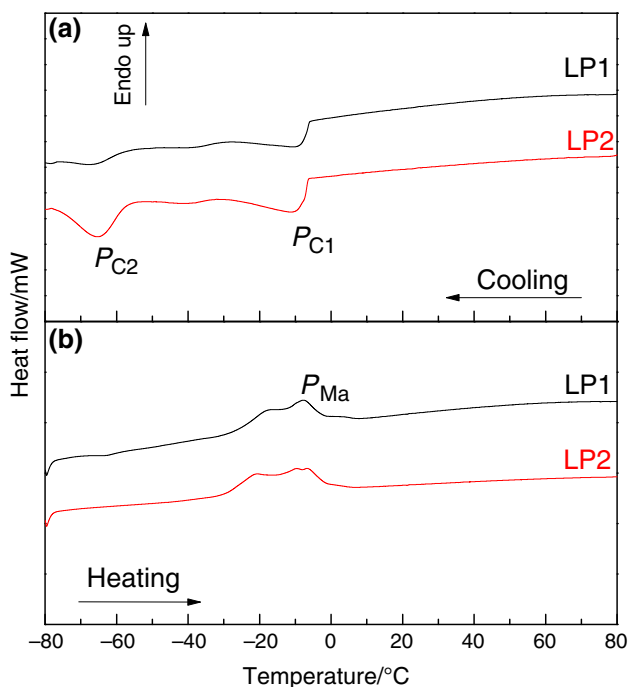

Fig. 4 Representative DSC curves of sapucaia oils. **a** DSC crystallization curve during cooling from 80 to − 80 °C. **b** DSC melting curve during heating from − 80 to 80 °C

Table 6 DSC parameters obtained from the transition phase of curves during crystallization (cooling) and melting (heating) curves of sapucaia nut oils

Sample	Cooling treatment (crystallization)												Heating treatment (melting)				
	Peak 1				Peak 2								Peak 1				
	Temperatures/°C			$\Delta H/$ J g^{-1}	Temperatures/°C			$\Delta H/$ J g^{-1}	$\Delta H/$ J g^{-1}	Temperature/ °C		Temperatures/°C			$\Delta H/$ J g^{-1}	R_{TM}
	T_o	P_{C1}	T_e	R	ΔH_{C1}	T_o	P_{C2}	T_e	R	ΔH_{C2}	ΔH_T	R_{TC}	T_o	P_M	T_e	R	ΔH_{TM}	
LP1	−8.04	−11.56	−23.20	15.16	−19.16	−59.80	−66.30	−73.93	14.13	−3.01	−22.17	−5.22 to −76.01	−25.77	−7.99	−1.68	24.09	59.34	−31.46 to 8.28
LP2	−8.43	−12.51	−31.47	23.04	−20.00	−65.15	−58.07	−73.92	8.77	−12.56	−32.56	−6.17 to −74.92	−29.87	−10.13	−1.09	28.78	64.76	−31.34 to 6.29

ΔH_{C1} and ΔH_{C2} = crystallization enthalpy for peak 1 and peak 2, respectively; ΔH_{TC} = total crystallization enthalpy; ΔH_{TM} = total melting enthalpy; P_{C1} = temperature of the first peak of the crystallization phase; P_{C2} = temperature of the second peak of the crystallization phase; P_M = temperature of the major peak of the melting phase; T_o and T_e = initial and end temperature of the transition phase, respectively; R = range of the transition phase (temperature difference between T_o and T_e); R_{TC} = total range of the crystallization transition phase; R_{Tm} = total range of the melting transition phase
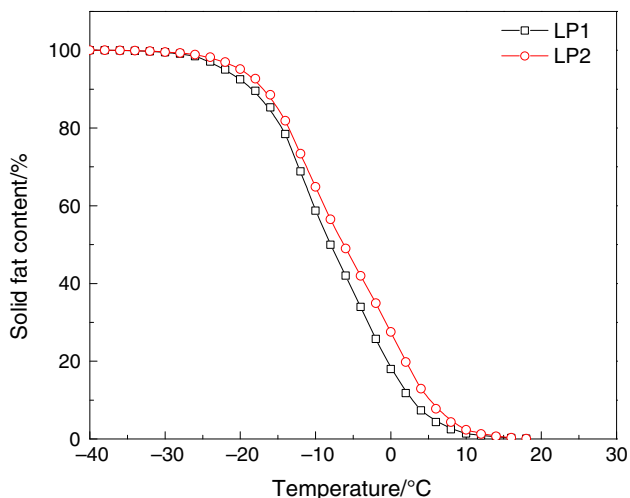
Fig. 5 Solid fat content of sapucaia oils measured by DSC

different shapes of the endothermic peaks [18]. The phase transitions are principally determined by the degree of heterogeneity in the composition of the oils and include the breaking and formation of hydrogen bonds, which is a

result of structural rearrangements in the chains of glycerides [51]. Major changes in the melting point are related to the formation of new TAG molecular species, such as desaturated and trisaturated TAG [31]. These results about the melting behavior of SO are important principally in the occasion in which is necessary to change some physicochemical properties to achieve specific functionalities for certain applications, such as the case of solid fats (e.g., margarine).

Solid fat content

The solid fat content (SFC) is considered an important physical property of lipids because it expresses their sensorial, technological and protecting/release properties, as well as their physical properties such as consistency, spreadability and stability [52]. According to the melting curves (Fig. 4b), SO presented no changes in SFC before − 40 °C, so the data analysis was performed in the range of − 40 to 20 °C (melting peak region). The SFC showed a less than 2.5% decrease between − 40 and − 30 °C for the two oils, then started to drop rapidly at around − 20 °C up

Table 7 Rheological parameters fitted to the Ostwald–de Waele and Herschel–Bulkley models for sapucaia nut oils at different temperatures

Sample	Temperature/°C	Ostwald–de Waele parameters			
		K /Pa s^n	n	R^2	χ^2
LP1	10	0.0801 ± 0.0041	0.9825 ± 0.0091	0.99999	0.00061
	20	0.0462 ± 0.0053	0.9936 ± 0.0030	0.99999	0.00044
	30	0.0328 ± 0.0001	0.9943 ± 0.0019	0.99999	0.00006
	40	0.0218 ± 0.0003	0.9906 ± 0.0035	0.99999	0.00005
	50	0.0160 ± 0.0001	0.9897 ± 0.0030	0.99999	0.00004
LP2	10	0.0598 ± 0.0059	0.9723 ± 0.0141	0.99961	0.01236
	20	0.0388 ± 0.0030	0.9841 ± 0.0105	0.99995	0.00087
	30	0.0293 ± 0.0008	0.9877 ± 0.0009	0.99983	0.00155
	40	0.0201 ± 0.0007	0.9966 ± 0.0001	0.99995	0.00026
	50	0.0125 ± 0.0007	0.9804 ± 0.0053	0.99995	0.00008

Sample	Temperature/°C	Herschel–Bulkley parameters				
		τ_{0H} /Pa$^{1/2}$	K_H /Pa s$^{1/2}$	n_H	R^2	χ^2
LP1	10	0.0251 ± 0.0008	0.0788 ± 0.0041	0.9851 ± 0.0092	0.99999	0.00028
	20	0.0212 ± 0.0162	0.0452 ± 0.0045	0.9971 ± 0.0005	0.99999	0.00013
	30	0.0072 ± 0.0009	0.0324 ± 0.0002	0.9960 ± 0.0017	0.99999	0.00003
	40	0.0068 ± 0.0011	0.0214 ± 0.0002	0.9931 ± 0.0031	0.99999	0.00003
	50	0.0060 ± 0.0009	0.0157 ± 0.0001	0.9928 ± 0.0025	0.99999	0.00002
LP2	10	0.1434 ± 0.0195	0.0521 ± 0.0043	0.9941 ± 0.0115	0.99996	0.00132
	20	0.0365 ± 0.0073	0.0370 ± 0.0033	0.9920 ± 0.0123	0.99999	0.00015
	30	0.0518 ± 0.0036	0.0268 ± 0.0006	1.0024 ± 0.0002	0.99999	0.00011
	40	0.0198 ± 0.0026	0.0191 ± 0.0006	1.0043 ± 0.0008	0.99999	0.00005
	50	0.0114 ± 0.0006	0.0119 ± 0.0007	0.9882 ± 0.0059	0.99999	0.00001

K, K_H = consistency coefficients; n, n_H = flow behavior indices (dimensionless); τ_{0H} = Herschel–Bulkley yield stress; R^2 = coefficient of determination; χ^2 = Chi-square

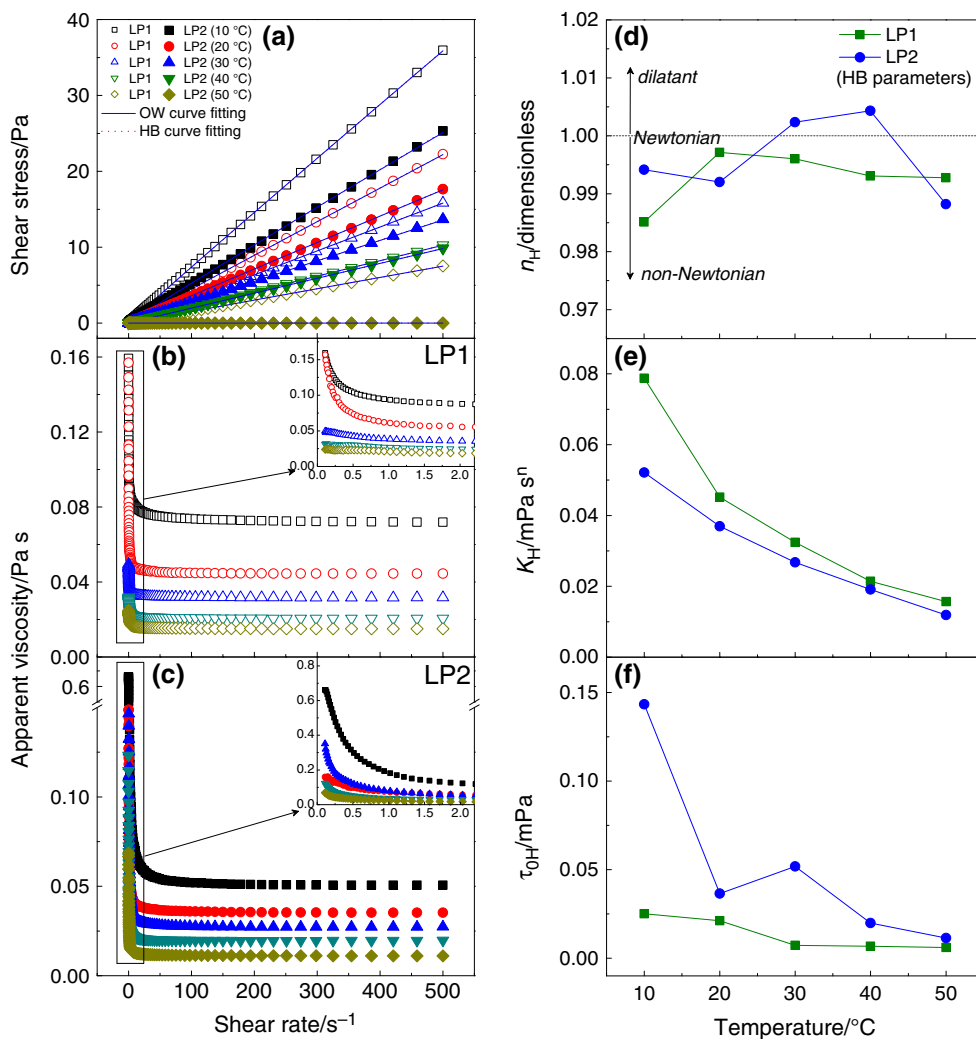**Fig. 6** Flow curves for sapucaia oils fitted by Ostwald–de Waele (solid line) and Herschel–Bulkley (dotted line) models (**a**); viscosity curves for LP1 (**b**, open symbols) and LP2 (**c**, filled symbols), recorded at 10, 20, 30, 40 and 50 °C; the evolution of HB parameters according to the temperature for flow index (**d**), consistency index (**e**) and yield stress (**f**)

to 0 °C and finally slowed down from 6 to 10 °C until there was no solid fat remaining (Fig. 5). The SFC is associated with the FA profile. Oils with higher UFA content are easier to melt than oils with higher SFA [48, 52].

Rheology properties

Steady-state rheology

The results for the rheological behavior of SO showed that the apparent viscosity (η) tends to decrease with increasing temperature (T) and also with increasing shear rate (γ), indicating that the flow of the sapucaia oils is pseudoplastic ($n > 1$) (Table 7, Fig. 6). On the one hand, it is usual for oils to exhibit a dependency on T; on the other hand, a non-dependency on γ at higher values is observed. At 50 °C, the

η is almost constant throughout the entire range tested, with a minimum impact of γ. Furthermore, 2.0 s^{-1} was the maximum value of γ that induced major changes in η (see detail in Fig. 6b, c). According to Gila et al. [53], a greater quantity of FAs such as C18:1 and C18:2 appear to make a great contribution to the flow behavior of oils.

The Ostwald–de Waele (OW) and Herschel–Bulkley (HB) models (Fig. 6a, Table 7) showed a good fit to the experimental data ($R^2 > 0.999$; $\chi^2 < 0.012$). In agreement with η, as T increased, the K and K_H values decreased (Fig. 6e, Table 7). A similar observation for many edible oils such as coconut, sunflower, canola, corn [54] and olive oils [55] has been reported. The OW model showed that the oils were non-Newtonian ($n < 1$) over the T range tested. However, the HB model revealed that sample LP2 behaved as a dilatant fluid ($n_H > 1$) at 30 and 40 °C (Fig. 6f). The HB model is able to
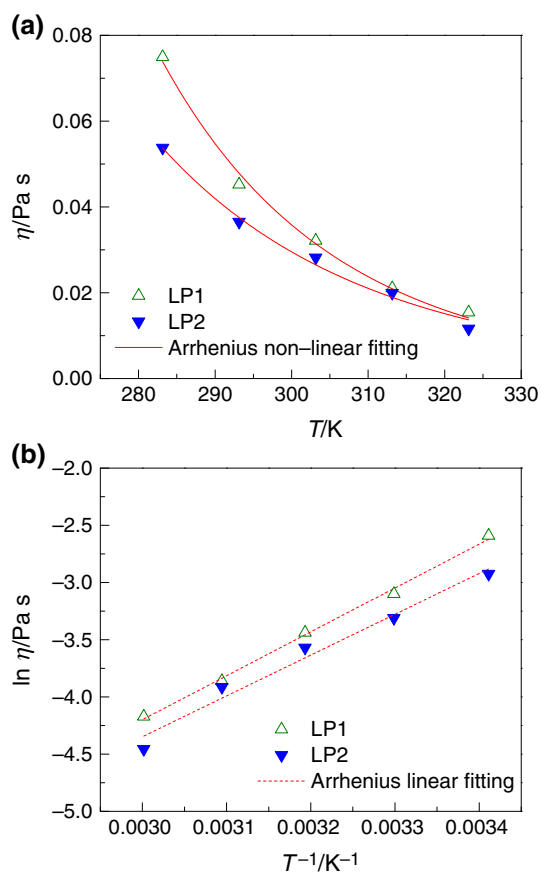
Fig. 7 The dependence of viscosities on temperature and the fit of the model to experimental data using the nonlinear Arrhenius equation (**a**) and the linearized Arrhenius equation (**b**) for sapucaia oils at different temperatures

determine the yield stress (τ_{0H}) at which a material begins to deform plastically without returning to its original shape when the applied stress is removed. SO had small values for τ_{0H}, which also tends to decrease with an increase in T.

Figure 7 shows the nonlinear and linear relationship of η versus T and ln η versus 1/T, respectively, obtained from the Arrhenius equation (Eq. 3) and fitted to experimental data (Table 8), illustrating the dependence of η on T. This could be due to the energy obtained to overcome the resistance to flow, which may, in turn, be due to the attractive forces among the oil molecules. This behavior is common for vegetable oils such as coconut oil, crude palm kernel oil, olive oil, sesame oil, soy oil and sunflower oil [56].

In vegetable oils, E_a is related to the PUFA content. Usually, a high poly-unsaturation (linoleic and linolenic acid content) would decrease, and high oleic content in the FA chain would increase, the E_a for oxidation [46]. Higher activation energy (E_a) values indicate the greater sensitivity of viscosity of the sample when the temperature is modified. In addition, the higher the E_a, the higher the stability to oxidation. The E_a for LP1 was slightly higher (31.89 kJ mol^{-1}) than LP2 (29.66 kJ mol^{-1}); therefore, LP1 produced greater variation in η in response to changes in T.

Oscillatory rheology

Viscoelasticity provides valuable information on the behavior of oils in relation to their composition and other physical properties. The storage modulus G' is correlated with elasticity (solid-like), whereas the loss modulus G'' is associated with viscosity (liquid-like). The complex modulus $|G^*|$ reveals the overall structure of the system, while the phase angle δ suggests whether a fat system is more solid-like or liquid-like [57].

In SO, there was a gradual decrease in $|G^*|$ during heating, followed by the opposite effect during cooling (Fig. 8a). This potentially revealed the destruction of a primary crystal network (melting effect) that was crystallized again when the oil was cooled, once $|G^*|$ returned to its initial values, thus strengthening the possible crystal network that was about to form again close to 10 °C [57]. In all samples, the elastic (G') and viscous (G'') components increased with the applied frequency over the range of 0.1–10 Hz, with G'' always being higher than G' (Fig. 8b, c). Therefore, the samples were all viscoelastic fluids with a predominant viscous component. Similar behavior has been reported for olive pomace oils [55].

Table 8 Comparison between activation energy (E_a) and the apparent viscosity (η) at a shear rate of 53.4 s^{-1} of sapucaia nut oils analyzed at different temperatures

Sample	E_a /kJ mol^{-1}	R^2	Apparent viscosity/Pa s				
			10 °C	20 °C	30 °C	40 °C	50 °C
LP1	31.89 ± 0.55[a]	0.989	0.0750 ± 0.0011[a]	0.0452 ± 0.0048[a]	0.0322 ± 0.0004[a]	0.0211 ± 0.0000[a]	0.0154 ± 0.0000[a]
LP2	29.66 ± 0.39[b]	0.978	0.0538 ± 0.0029[b]	0.0365 ± 0.0013[b]	0.0282 ± 0.0006[b]	0.0200 ± 0.0007[b]	0.0116 ± 0.0004[b]

Means followed by same letter do not differ by Duncan test ($p < 0.05$)

ATR-FTIR analysis

In Fig. 9, each peak corresponds to a functional group responsible for IR absorption; the intensities of each peak are associated with the concentration of functional groups present in both oils. To the naked eye, the entire range of spectra looks very similar for each SO. There are no considerable differences between their spectral features apart from slight changes in the absorbances of some bands as well as some shifts in the exact position of the bands. In general, the spectra displayed the characteristic peaks of
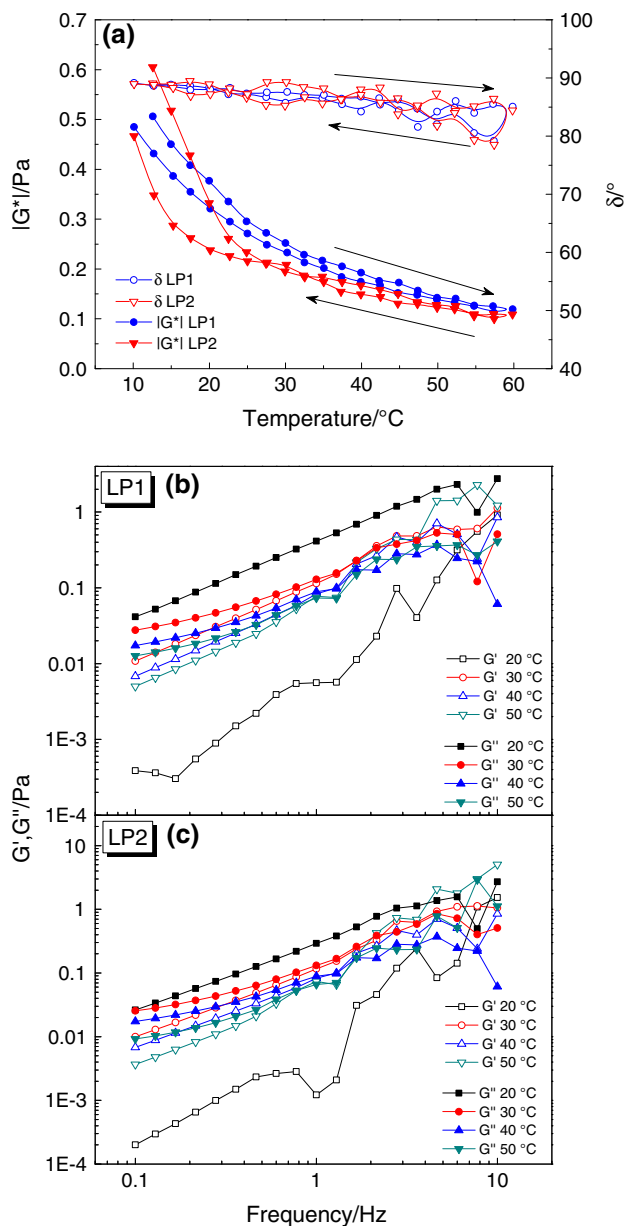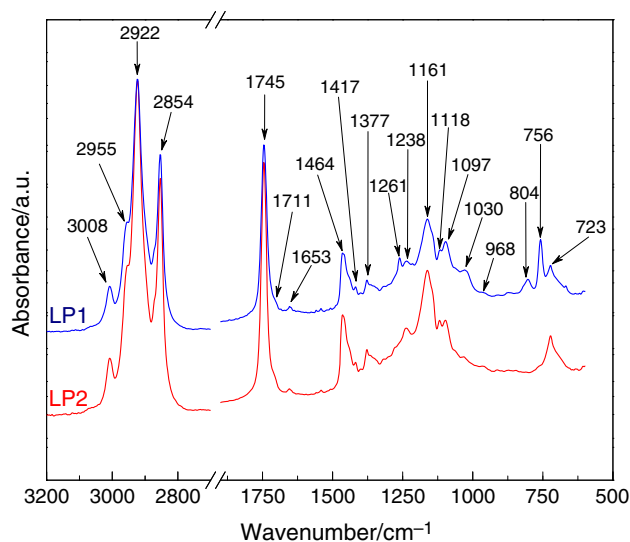
Fig. 9 ATR-FTIR spectra of sapucaia oils measured in mid-IR regions of 4000–650 cm^{-1}

functional groups common to ester samples [51, 58]. Some differences were observed only at the absorption bands around 2955, 1261, 804 and 756 cm^{-1} (Table 9).

Peaks in the region of 3008 cm^{-1}, attributed to *cis* –C=CH vibration, and at 1653 cm^{-1}, caused by vibration of *cis* C=C, were present in both samples. This peak is also correlated with the presence of UFAs [51, 58, 59].

The strong bands at around 2922 and 2854 cm^{-1} can be ascribed to the asymmetric and symmetric C–H stretching vibrations of CH_2 groups, which are also present in macaúba palm (*Acrocomia aculeata*) oils [51]. The triglyceride, which is a major component of edible oils and fats, was dominant in the spectra. The major peaks that represent triglyceride functional groups could be observed around 2922, 2854, 1745, 1464, 1161 and 723 cm^{-1} [59].

A small shoulder at 1711 cm^{-1} was also detected and assigned to free FAs. The band at 1464 cm^{-1} is the scissoring band of the bending vibration of the methylene group. A band at 1417 cm^{-1} was attributed to rocking vibrations of CH bonds of *cis*-disubstituted olefins [59]. Likewise, a band at 1377 cm^{-1} could be due to the symmetric bending vibration of methyl groups. The band at around 1161 cm^{-1} could be assigned to the stretching of the C–O bonds of aliphatic esters or CH_2 bending vibrations [60]. In addition, the peak at 1161 cm^{-1} and its shoulder at 1238 cm^{-1} were considered as fingerprints of C–O stretching in long-chain fatty acids [23]. The sapucaia oils presented a small peak in the region of 968 cm^{-1}, which was assigned to *trans* UFAs. Finally, the band at 722 cm^{-1} was attributed to $(CH_2)_n$ rocking [59].

These differences between the FTIR spectra of LP1 and LP2 confirm that the extraction method caused some alterations to the chemical profile of the oils. This finding

Fig. 8 Temperature sweep during heating (10–60 °C) and cooling (60–10 °C) (**a**) and a frequency sweep of sapucaia oils obtained by Bligh and Dyer (**b**) and by Soxhlet (**c**) extractions

Table 9 Absorption bands in the ATR-FTIR spectra of the sapucaia nut oils

Wavenumber/cm^{-1}		Functional group	Mode of vibration[a]
LP1	LP2		
3008	3008	=C–H (*cis-*)	Stretching
2955	2953	–C–H (CH$_3$)	Stretching (asymmetric)
2922	2922	–C–H (CH$_2$)	Stretching (asymmetric)
2854	2854	–C–H (CH$_2$)	Stretching (symmetric)
1745	1745	–C=O (ester)	Stretching
1711	1711	–C=O (acid)	Stretching
1653	1653	–C=C–(*cis-*)	Stretching
1464	1464	–C–H (CH$_2$, CH$_3$)	Bending (scissoring)
1417	1417	=C–H (*cis-*)	Bending (rocking)
1377	1377	–C–H (CH$_3$)	Bending (symmetric)
1261	–	–C–O	Stretching
1238	1238	–C–O, –CH$_2$–	Stretching, bending
1161	1161	–C–O, –CH$_2$–	Stretching, bending
1118	1118	–C–O	Stretching
1097	1097	–C–O	Stretching
1030	1030	–C–O	Stretching
968	968	–HC=CH–(*trans-*)	Bending out of plane
914	914	–HC=CH–(*cis-*)	Bending out of plane
804	–	–C–H	Bending out of plane
756	–	–C–H	Bending out of plane
723	723	–(CH$_2$)$_n$–,–HC=CH–(*cis-*)	Bending (rocking)

[a]From Guillen and Cabo [59]

also suggests that oil composition can affect the exact position of the bands and also affects the shifts in the IR spectra.

Conclusions

The thermal and rheological properties, oxidative stability, antioxidant activity and FTIR spectroscopy analysis of oils from sapucaia nuts (SO) were studied, and the results are reported here for the first time. The analyses indicated that the method of extraction impacts the fatty acid composition of the oils. SO present high UFA/SFA relationship regardless of the extraction process, but the linoleic/oleic FA ratio is highly affected by the extraction method. Furthermore, the oil extracts presented considerable total phenolic compounds content and antioxidant properties. The type of oil extraction also had a minor impact on the rheological behavior and clearly affects the plasticity of the oils. Ostwald–de Waele and Herschel–Bulkley models indicated that the oils exhibit major pseudoplastic

behavior. The effect of temperature on the changes in viscosity was found to be more significant than the effect of shear rate. Thermal analysis indicated that the sapucaia oils were thermally stable up to 300 °C with $\sim$ 5% mass loss. The DSC parameters showed that the melting profiles of sapucaia oils are similar regardless of the method of extraction. The oxidative stability index of *L. pisonis* oils was established by Rancimat. The oils presented similar FTIR patterns, with characteristic bands for vegetable oils. These results reinforce the idea that sapucaia oils are suitable for human consumption. In addition, these data open up new possibilities for the industrial utilization of these oils for food, cosmetic and pharmaceutical industries and also for the production of biodiesel. Further research is needed to investigate other chemical compounds of these oils, such as tocopherols, and their potential biological activities.

References

1. Reuters T. Web of science. Web Sci. 2017 [cited 2017 Feb 2]. https://webofknowledge.com/.
2. Berto A, da Silva AF, Visentainer JV, Matsushita M, de Souza NE. Proximate compositions, mineral contents and fatty acid compositions of native Amazonian fruits. Food Res Int. 2015;77:441–9. doi:10.1016/j.foodres.2015.08.018.
3. Naozuka J, Carvalho Vieira E, Nascimento AN, Oliveira PV. Elemental analysis of nuts and seeds by axially viewed ICP OES. Food Chem. 2011;124:1667–72. doi:10.1016/j.foodchem.2010.07.051.
4. Oliveira VB, Yamada LT, Fagg CW, Brandão MGL. Native foods from Brazilian biodiversity as a source of bioactive compounds. Food Res Int. 2012;48:170–9. doi:10.1016/j.foodres.2012.03.011.
5. Costa T, Jorge N. Characterization and fatty acids profile of the oils from Amazon nuts and walnuts: characterization and fatty acids profile of the oilseeds. Nutr Food Sci. 2012;42:279–87. doi:10.1108/00346651211248647.
6. Queiroga Neto V, Bora PS, Diniz ZN, Cavalheiro JMO, Queiroga KF. *Dipteryx lacunifera* seed oil: characterization and thermal stability. Ciênc Agrotecnol. 2009;33:1601–7. doi:10.1590/S1413-70542009000600020.
7. da Costa PA, Ballus CA, Teixeira-Filho J, Godoy HT. Phytosterols and tocopherols content of pulps and nuts of Brazilian fruits. Food Res Int. 2010;43:1603–6. doi:10.1016/j.foodres.2010.04.025.

8. Wickens GE. Edible nuts. Non-wood For. Prod. Rome: Food and Agriculture Organization of the United Nations; 1995. p. 198. http://www.fao.org/docrep/018/v8929e/v8929e.pdf.

9. Rodrigues AB, Florence CT, Mariano-Neto E, Gaiotto FA. First microsatellite markers for *Lecythis pisonis* (Lecythidaceae), an important resource for Brazilian fauna. Conserv Genet Resour. 2015;7:437–9. doi:10.1007/s12686-014-0390-6.

10. Vallilo MI, Tavares M, Aued-Pimentel S, Campos NC. Neto JMM. *Lecythis pisonis* Camb. nuts: oil characterization, fatty acids and minerals. Food Chem. 1999;66:197–200. doi:10.1016/S0308-8146(99)00040-0.

11. Carvalho MG, Costa JMC, Souza VAB, Maia GA. Avaliação dos parâmetros físicos e nutricionais de amêndoas de sapucaia and castanha-do-gurguéia. Rev Ciênc Agron. 2008;39:517–23.

12. de Carvalho IMM, Queirós LD, Brito LF, Santos FA, Bandeira AVM, de Souza AL, et al. Caracterização química da castanha de sapucaia (*Lecythis pisonis* Cambess.) da região da zona da mata Mineira. Biosci J. 2012;28:971–7.

13. Denadai SMS, Hiane PA, Marangoni S, Baldasso PA, Miguel AMRDO, Macedo MLR. In vitro digestibility of globulins from sapucaia (*Lecythis pisonis* Camb.) nuts by mammalian digestive proteinases. Ciênc Tecnol Aliment. 2007;27:535–43.

14. Brandão MS, Pereira SS, Lima DF, Oliveira JPC, Ferreira ELF, Chaves MH, et al. Antinociceptive effect of *Lecythis pisonis* Camb. (Lecythidaceae) in models of acute pain in mice. J Ethnopharmacol. 2013;146:180–6.

15. Silva LL, Gomes BS, Sousa-Neto BP, Oliveira JPC, Ferreira ELF, Chaves MH, et al. Effects of *Lecythis pisonis* Camb. (Lecythidaceae) in a mouse model of pruritus. J Ethnopharmacol. 2012;139:90–7. doi:10.1016/j.jep.2011.10.023.

16. Ferreira ÉLDF, Mascarenhas TS, Oliveira JPDC, Chaves MH, Araújo BQ, Cavalheiro AJ. Phytochemical investigation and antioxidant activity of extracts of *Lecythis pisonis*. Camb J Med Plants Res. 2014;8:353–6016. doi:10.5897/JMPR2013.5153.

17. Vieira MEB, Vasconcelos IM, Machado OLT, Gomes VM, Carvalho ADO. Isolation, characterization and mechanism of action of an antimicrobial peptide from *Lecythis pisonis* seeds with inhibitory activity against *Candida albicans*. Acta Biochim Biophys Sin. 2015;47:716–29. doi:10.1093/abbs/gmv071.

18. Samyn P, Schoukens G, Vonck L, Stanssens D, Van Den Abbeele H. Quality of Brazilian vegetable oils evaluated by (modulated) differential scanning calorimetry. J Therm Anal Calorim. 2012;110:1353–65. doi:10.1007/s10973-011-2132-2.

19. Teixeira GL, Züge LCB, Silveira JLM, Scheer ADP, Ribani RH. The impact of polyoxyethylene sorbitan surfactants in the microstructure and rheological behaviour of emulsions made with melted fat from Cupuassu (*Theobroma grandiflorum*). J Surfactants Deterg. 2016;19:725–38. doi:10.1007/s11743-016-1820-0.

20. AOCS. Official methods and recommended practices of the American OIL Chemists' Society. 5th ed. Champaign: AOCS Press; 1997.

21. Mettler Toledo. Good titration practice in Karl Fischer titration. 2013. http://fr.mt.com/dam/LabDiv/Campaigns/TestingLabs2013/moisture/package/gtp-karl-fischer-EN.pdf.

22. Pena Muniz MA, dos Santos MNF, da Costa CEF, Morais L, Lamarão MLN, Ribeiro-Costa RM, et al. Physicochemical characterization, fatty acid composition, and thermal analysis of *Bertholletia excelsa* HBK oil. Pharmacogn Mag. 2015;11:147–51. doi:10.4103/0973-1296.149730.

23. Zhang X, Li L, Xie H, Liang Z, Su J, Liu G, et al. Comparative analysis of thermal behavior, isothermal crystallization kinetics and polymorphism of palm oil fractions. Molecules. 2013;18:1036–52. doi:10.3390/molecules18011036.

24. Menard KF, Sichina WJ. Prediction of solid fat index (SFI) values of food fats using DSC. Perkin Elmer Appl Note. Waltham: Perkin Elmer; 2000.

25. Bail S, Stuebiger G, Krist S, Unterweger H, Buchbauer G. Characterisation of various grape seed oils by volatile compounds, triacylglycerol composition, total phenols and antioxidant capacity. Food Chem. 2008;108:1122–32. doi:10.1016/j.foodchem.2007.11.063.

26. Sánchez-Rangel JC, Benavides J, Heredia JB, Cisneros-Zevallos L, Jacobo-Velázquez DA. The Folin–Ciocalteu assay revisited: improvement of its specificity for total phenolic content determination. Anal Methods. 2013;5:5990–9. doi:10.1039/c3ay41125g.

27. Brand-Williams W, Cuvelier ME, Berset C. Use of a free radical method to evaluate antioxidant activity. LWT Food Sci Technol. 1995;28:25–30. doi:10.1016/S0023-6438(95)80008-5.

28. Re R, Pellegrini N, Proteggente A, Pannala A, Yang M, Rice-Evans C. Antioxidant activity applying an improved ABTS radical cation decolorization assay. Free Radic Biol Med. 1999;26:1231–7. doi:10.1016/S0891-5849(98)00315-3.

29. Benzie I, Strain J. The ferric reducing ability of plasma (FRAP) as a measure of "antioxidant power": the FRAP assay. Anal Biochem. 1996;239:70–6. doi:10.1006/abio.1996.0292.

30. Zielinski AAF, Haminiuk CWI, Beta T. Multi-response optimization of phenolic antioxidants from white tea (*Camellia sinensis* L. Kuntze) and their identification by LC-DAD-Q-TOF-MS/MS. LWT Food Sci Technol. 2016;65:897–907. doi:10.1016/j.lwt.2015.09.020.

31. Guedes AMM, Antoniassi R, Galdeano MC, Grimaldi R, De Carvalho MG, Wilhelm AE, et al. Length-scale specific crystalline structural changes induced by molecular randomization of pequi oil. J Oleo Sci. 2017;66:469–78. doi:10.5650/jos.ess16192.

32. Ghazani SM, Marangoni AG. Minor components in canola oil and effects of refining on these constituents: a review. JAOCS. J Am Oil Chem Soc. 2013;90:923–32. doi:10.1007/s11746-013-2254-8.

33. Van Hoed V. Phenolic compounds in seed oils. Lipid Technol. 2010;22:247–9. doi:10.1002/lite.201000063.

34. Miraliakbari H, Shahidi F. Antioxidant activity of minor components of tree nut oils. Food Chem. 2008;111:421–7. doi:10.1016/j.foodchem.2008.04.008.

35. Castelo-Branco VN, Santana I, Di-Sarli VO, Freitas SP, Torres AG. Antioxidant capacity is a surrogate measure of the quality and stability of vegetable oils. Eur J Lipid Sci Technol. 2016;118:224–35. doi:10.1002/ejlt.201400299.

36. Christodouleas DC, Fotakis C, Nikokavoura A, Papadopoulos K, Calokerinos AC. Modified DPPH and ABTS assays to assess the antioxidant profile of untreated oils. Food Anal Methods. 2015;8:1294–302. doi:10.1007/s12161-014-0005-6.

37. Blomhoff R, Carlsen MH, Andersen LF, Jacobs DR Jr. Health benefits of nuts: potential role of antioxidants. Br J Nutr. 2006;96:S52–60. doi:10.1017/BJN20061864.

38. Castelo-Branco VN, Torres AG. Potential application of antioxidant capacity assays to assess the quality of edible vegetable oils. Lipid Technol. 2009;21:152–5. doi:10.1002/lite.200900035.

39. Malacrida CR, Kimura M, Jorge N. Phytochemicals and antioxidant activity of citrus seed oils. Food Sci Technol Res. 2012;18:399–404. doi:10.3136/fstr.18.399.

40. Huang D, Boxin OU, Prior RL. The chemistry behind antioxidant capacity assays. J Agric Food Chem. 2005;53:1841–56. doi:10.1021/jf030723c.

41. Mišurcová L, Ambrožová J, Samek D. Seaweed lipids as nutraceuticals. Adv Food Nutr Res. 2011;64:339–55. doi:10.1016/B978-0-12-387669-0.00027-2.

42. Costa-Singh T, Bitencourt TB, Jorge N. Caracterização e compostos bioativos do óleo da castanha-de-cutia (*Couepia edulis*). Rev Inst Adolfo Lutz. 2012;71:61–8.

43. Orsavova J, Misurcova L, Ambrozova J, Vicha R, Mlcek J. Fatty acids composition of vegetable oils and its contribution to dietary energy intake and dependence of cardiovascular mortality on dietary intake of fatty acids. Int J Mol Sci. 2015;16:12871–90. doi:10.3390/ijms160612871.

44. Siger A, Nogala-Kalucka M, Lampart-Szczapa E. The content and antioxidant activity of phenolic compounds in cold-pressed plant oils. J Food Lipids. 2008;15:137–49. doi:10.1111/j.1745-4522.2007.00107.x.

45. Queiroga Neto V, Bakke OA, Ramos CMP, Bora PS, Letelier JC, Conceição MM. Brazil Nut (*Bertholletia excelsa* HBK) seed kernel oil: characterization and thermal stability. Rev Bras Biol Farm. 2009;3:33–42.

46. Tengku-Rozaina TM, Birch EJ. Thermal oxidative stability analysis of hoki and tuna oils by differential scanning calorimetry and thermogravimetry. Eur J Lipid Sci Technol. 2016;118:1053–61. doi:10.1002/ejlt.201500310.

47. Gao F, Birch J. Oxidative stability, thermal decomposition, and oxidation onset prediction of carrot, flax, hemp, and canola seed oils in relation to oil composition and positional distribution of fatty acids. Eur J Lipid Sci Technol. 2016;118:1042–52. doi:10.1002/ejlt.201500208.

48. Gao F, Yang S, Birch J. Physicochemical characteristics, fatty acid positional distribution and triglyceride composition in oil extracted from carrot seeds using supercritical CO_2. J Food Compos Anal. 2016;45:26–33. doi:10.1016/j.jfca.2015.09.004.

49. Li R, Huang J, Huang L, Teng J, Xia N, Wei B, et al. Comparison of GC and DSC monitoring the adulteration of camellia oil with selected vegetable oils. J Therm Anal Calorim Springer Neth. 2016;126:1735–46.

50. Tan CP, Che Man YB. Differential scanning calorimetric analysis of edible oils: comparison of thermal properties and chemical composition. J Am Oil Chem Soc. 2000;77:143–55. doi:10.1007/s11746-000-0024-6.

51. Del Río JC, Evaristo AB, Marques G, Martín-Ramos P, Martín-Gil J, Gutiérrez A. Chemical composition and thermal behavior of the pulp and kernel oils from macauba palm (*Acrocomia aculeata*) fruit. Ind Crops Prod. 2016;84:294–304. doi:10.1016/j.indcrop.2016.02.018.

52. Augusto PED, Soares BMC, Chiu MC, Gonçalves LAG. Modelling the effect of temperature on the lipid solid fat content (SFC). Food Res Int. 2012;45:132–5. doi:10.1016/j.foodres.2011.10.026.

53. Gila A, Jiménez A, Beltrán G, Romero A. Correlation of fatty acid composition of virgin olive oil with thermal and physical properties. Eur J Lipid Sci Technol. 2015;117:366–76. doi:10.1002/ejlt.201400078.

54. Wan Nik WB, Ani FN, Masjuki HH, Eng Giap SG. Rheology of bio-edible oils according to several rheological models and its potential as hydraulic fluid. Ind Crops Prod. 2005;22:249–55. doi:10.1016/j.indcrop.2005.01.005.

55. Sánchez-Gutiérrez CA, Casas M, Lucero MJ, Ruiz-Méndez MV. Physico-chemical and rheological characterization of olive-pomace oils. Eur J Lipid Sci Technol. 2015;117:87–91. doi:10.1002/ejlt.201300490.

56. Giap SGE. The hidden property of arrhenius-type relationship: viscosity as a function of temperature. J Phys Sci. 2010;21:29–39.

57. Xu Y, Wei C, Zhao X, Lu C, Dong C. A comparative study on microstructure, texture, rheology, and crystallization kinetics of palm-based diacylglycerol oils and corresponding palm-based oils. Eur J Lipid Sci Technol. 2016;118:1179–92. doi:10.1002/ejlt.201500369.

58. Rohman A, Che Man YB. Simultaneous quantitative analysis of two functional food oils, extra virgin olive oil and virgin coconut oil using FTIR spectroscopy and multivariate calibration. Int Food Res J. 2011;18:1231–5.

59. Guillén MD, Cabo N. Characterization of edible oils and lard by fourier transform infrared spectroscopy. Relationships between composition and frequency of concrete bands in the fingerprint region. J Am Oil Chem Soc. 1997;74:1281–6. doi:10.1002/(SICI)1097-0010(199709)75:1<1:AID-JSFA842>3.0.CO;2-R.

60. Zhang H, Ma J, Miao Y, Tuchiya T, Chen JY. Analysis of carbonyl value of frying oil by fourier transform infrared spectroscopy. J Oleo Sci. 2015;64:375–80. doi:10.5650/jos.ess14201.